Fundamental and Second-Order Superregular Breathers in Vector Fields

Chong Liu,[1,2,3,4,*] Shao-Chun Chen,[1] and Nail Akhmediev[2,†]

[1]*School of Physics, Northwest University, Xi'an 710127, China*
[2]*Department of Fundamental and Theoretical Physics, Research School of Physics,*
The Australian National University, Canberra, Australian Capital Territory 2600, Australia
[3]*Shaanxi Key Laboratory for Theoretical Physics Frontiers, Xi'an 710127, China*
[4]*Peng Huanwu Center for Fundamental Theory, Xi'an 710127, China*

We developed an exact theory of the superregular breathers (SRBs) of Manakov equations. We have shown that the vector SRBs do exist both in the cases of focusing and defocusing Manakov systems. The theory is based on the eigenvalue analysis and on finding the exact links between the SRBs and modulation instability. We have shown that in the focusing case the localized periodic initial modulation of the plane wave may excite both a single SRB and the second-order SRBs involving four fundamental breathers.

Understanding the formation of oscillating localized structures known as "breathers" is a fundamental problem in a wide variety of conservative and dissipative systems [1–7]. Breathers are known in optics [8], hydrodynamics [9], Bose-Einstein condensates [6], micromechanical arrays [10], and in the cavity optomechanics [11]. They provide a basis for more complicated formations— nonlinear superpositions of breathers that appear in many nonlinear phenomena of physical importance such as rogue wave events [12–14], breather molecules [15], chessboard-like patterns [16], breather turbulence [17], higher-order modulation instability (MI) [18,19], and the MI where small periodic modulation is additionally localized in transverse direction. The latter leads to the excitation of superregular breathers (SRBs) [20].

As it was shown in [20–22], the SRBs are higher-order exact solutions of the scalar nonlinear Schrödinger equation (NLSE) that consist of two fundamental breathers propagating at small angle to each other. Later, the ideas of SRB theory have been successfully applied to the NLSE with higher-order effects [23], complex modified KdV equation [24], equations modeling the resonant erbium-doped fiber [25], self-induced transparency [26], and the derivative NLSE [27]. One of the important results of these studies is that the MI growth rate related to the SRB excitation is defined by the absolute difference of group velocities of two breathers [28].

SRBs modeled by the scalar NLSE have been observed both in experiments in fiber optics and on water surface [22]. In each medium, the initial conditions required to excite the SRBs have been carefully modeled by the exact solutions. Further studies have shown that a larger variety of initial conditions also lead to their excitation [29–31]. So far, these studies are limited to the NLSE-type integrable systems with an associated 2×2 Lax pair. Extending this knowledge to the more complex systems consisting of two coupled wave fields still remains a challenge. One of the practically important cases involves Manakov equations [32]. These equations play a pivotal role in modeling variety of nonlinear wave phenomena in Bose-Einstein condensates [33], in optics [34–36], in hydrodynamics [37], and, perhaps, in finances [38].

Higher-order nonlinear excitations in coupled wave systems are under intense investigations [39,40]. It was found, in the earlier work [40], that MI does exist in defocusing Manakov system. Moreover, there are nontrivial vector analogs of the focusing scalar rogue wave solutions in the defocusing regime. It was also found, in [40], that taking different wave vectors are important for construction of new solutions that cannot be obtained simply transforming the scalar ones. Our present work confirms the above findings.

Several other studies in this direction have been made [41–43]. Certain types of vector breathers of the Manakov system (named vector breathers of types II and III) have been derived in [43]. As it was shown later in [42], these types of breathers cannot form SRB pairs. The complications arise because of the increased number of spectral parameters in vector breather solutions. Also, the practically important task of their excitation from weak modulations remains to be addressed.

We start with the Manakov equations in dimensionless form, which are given by

$$i \frac{\partial \psi^{(1)}}{\partial t} + \frac{1}{2} \frac{\partial^2 \psi^{(1)}}{\partial x^2} + \sigma \left(|\psi^{(1)}|^2 + |\psi^{(2)}|^2 \right) \psi^{(1)} = 0,$$
$$i \frac{\partial \psi^{(2)}}{\partial t} + \frac{1}{2} \frac{\partial^2 \psi^{(2)}}{\partial x^2} + \sigma \left(|\psi^{(1)}|^2 + |\psi^{(2)}|^2 \right) \psi^{(2)} = 0, \quad (1)$$

where $\psi^{(j)}$ ($j = 1$, 2) are the two nonlinearly coupled components of the vector wave field. Parameter $\sigma(=\pm 1)$ defines the strength of the nonlinear terms in Eqs. (1). It corresponds (in optics) to the self-focusing regime when $\sigma = +1$ and self-defocusing regime when $\sigma = -1$.

The fundamental breather solution can be constructed using Darboux transformation [44] (see Supplemental Material [45]):

$$\psi^{(j)} = \psi_0^{(j)}\big[1 - (1 + \sigma A)\psi_a^{(j)}\big], \qquad (2)$$

where $\psi_0^{(j)} = a_j \exp\{i\beta_j x + i[\sigma(a_1^2 + a_2^2) - \frac{1}{2}\beta_j^2]t\}$ is the vector plane wave of Eqs. (1) with a_j, and β_j being the plane wave amplitudes and wave numbers, respectively. Moreover, $A = \sum_{j=1}^2 \{a_j^2/[(\chi^* + \beta_j)(\chi + \beta_j)]\}$. χ is the eigenvalue that obeys the relation

$$1 + \sigma \sum_{j=1}^2 \frac{a_j^2}{(\chi + \beta_j)(\chi + \omega + 2i\gamma + \beta_j)} = 0, \qquad (3)$$

Parameters ω and γ determine the period and the width of the breather. Spatiotemporal evolution of the breather (2) is defined by the functions

$$\psi_a^{(j)} = 2i\chi_i \frac{\mathcal{B}^{(j)}(\chi)(e^\Gamma + e^{-i\Lambda}) + \mathcal{B}^{(j)}(\tilde{\chi})(e^{-\Gamma} + e^{i\Lambda})}{\varepsilon(\chi)e^\Gamma + \varepsilon(\tilde{\chi})e^{-\Gamma} + \mathcal{D}e^{i\Lambda} + \mathcal{D}^* e^{-i\Lambda}},$$

where $\tilde{\chi} = \chi + \omega + 2i\gamma$ and the arguments Γ and Λ are

$$\Gamma = 2\gamma\{x - V_g(\chi)t\}, \qquad \Lambda = \omega\{x - V_p(\chi)t\} - \theta_1.$$

Here, $x = x - x_{01}$, $t = t - t_{01}$ with x_{01} and t_{01} being responsible for the spatial and temporal position of the breather. θ_1 is an arbitrary phase, while V_g and V_p are the group and phase velocities:

$$V_g(\chi) = -\frac{\omega}{2\gamma}\chi_i - \omega - \chi_r, \qquad (4)$$

$$V_p(\chi) = \frac{2\gamma}{\omega}(\chi_i + \gamma) - \frac{\omega}{2} - \chi_r. \qquad (5)$$

Subscripts r and i denote the real and imaginary parts, respectively. The coefficients in $\psi_a^{(j)}$ are $\mathcal{B}^{(j)}(\chi) = 1/(\chi + \beta_j)$, $\varepsilon(\chi) = 1 + \sigma \sum_{j=1}^2 |a_j/(\beta_j + \chi)|^2$, and $\mathcal{D} = 1 + \sigma \sum_{j=1}^2 a_j^2/[(\beta_j + \chi^*)(\beta_j + \tilde{\chi})]$. The asterisk denotes complex conjugation. Here, we use $\beta_1 = -\beta_2 = \beta$. In order to simplify further our analysis, we take equal plane wave amplitudes $a_1 = a_2 = a = 1$.

The family of solutions (2) contains several subsets [46–52]. They are vector generalizations of Kuznetsov-Ma solitons [53], Akhmediev breathers (ABs) [54], and Peregrine solitons [55]. In particular, when $\gamma = 0$, implying $\Gamma = -\omega\chi_i t$, Eqs. (2) define the vector ABs. They are

localized in t but periodic in x with period $2\pi/\omega$. The AB is known as the nonlinear stage of MI developed from purely periodic modulation [54]. The MI growth rate described by the vector AB solution is given by

$$\mathcal{G} = |2\gamma V_g(\chi)| = |\omega\chi_{AB}|, \qquad \chi_{AB} \equiv \chi_i|_{\gamma=0}. \qquad (6)$$

At small but nonzero γ, Eqs. (2) describe vector quasi-ABs with finite envelope width $1/(2\gamma)$ in x. The period in x is still $2\pi/\omega$. The nonlinear superposition of a pair of quasi-ABs each with the period $2\pi/\omega$ and the width $1/(2\gamma)$ can form a SRB. In contrast to ABs, it evolves from MI with finite width of modulation.

Solution (2) requires further analysis. From Eq. (3), we have explicit expressions for the eigenvalues χ:

$$\chi_{1,3} = (\mu \mp \sqrt{\nu})^{1/2} - \alpha, \qquad \chi_{2,4} = -(\mu \mp \sqrt{\nu})^{1/2} - \alpha, \qquad (7)$$

where $\mu = \alpha^2 + \beta^2 - \sigma a^2$, $\nu = 4(\alpha\beta)^2 - 4\sigma(a\beta)^2 + a^4$, and $\alpha = \omega/2 + i\gamma$. The MI growth rate of the ABs, as follows from Eq. (6) is defined by $\chi_{AB}^{(\mp)}$. It is given by

$$i\chi_{AB}^{(\mp)} + \rho^{(\mp)} = (\mu \mp \sqrt{\nu})^{1/2}|_{\gamma=0}. \qquad (8)$$

The areas of parameters ω and β with nonzero growth rate $\mathcal{G}$ define the existence of the vector ABs and SRBs. These areas calculated using (6) and (8) are shown on the diagrams presented in Figs. 1(a) and 1(b) for the defocusing and the focusing cases, respectively. They are constructed using the Hessian matrix formalism [56]. The ABs and SRBs with various patterns do exist in the colored areas of these diagrams. These patterns can be described as periodic repetition of bright, dark, and four-petal structures observed in the ABs [56].
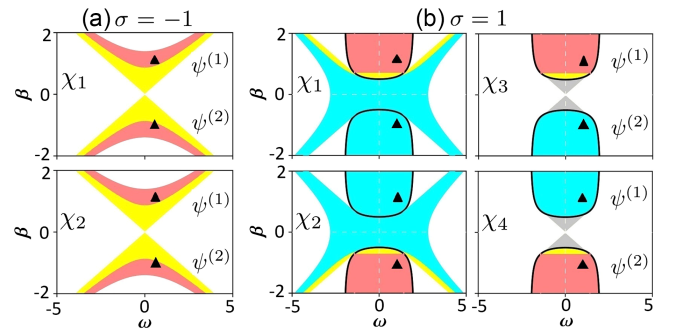

FIG. 1. Existence diagram for ABs and SRBs on (ω, β) plane when (a) $\sigma = -1$ and (b) $\sigma = 1$. Colored areas correspond to nonzero growth rate $\mathcal{G}$. The cyan, pink, and yellow areas correspond to the bright, dark, and four-petal patterns, respectively. Gray areas in (b) are invalid for AB and SRB formation. The solid lines in (b) correspond to $\nu|_{\gamma=0} = 0$. In each panel, $\psi^{(2)}(\beta) = \psi^{(1)}(-\beta)$. The solid triangles show the parameter values used in Figs. 2 and 3.

SRBs have slightly different eigenvalues and, consequently, the growth rates than the ABs. Expanding Eqs. (7) using the small parameter γ ($\gamma^2 \ll 1$), and separating the real and imaginary parts, in the first order, we have

$$\chi_{1,3i} = \mathcal{O}(\gamma^2) + \chi_{AB}^{(\mp)} - \gamma, \quad \chi_{1,3r} = \mathcal{O}(\gamma^2) + \rho^{(\mp)} - \omega,$$
$$\chi_{2,4i} = \mathcal{O}(\gamma^2) - \chi_{AB}^{(\mp)} - \gamma, \quad \chi_{2,4r} = \mathcal{O}(\gamma^2) - \rho^{(\mp)} - \omega. \quad (9)$$

The nonlinear superposition of one pair of quasi-ABs with two different eigenvalues (9) produces potentially a vector SRB. However, not every kind of combination of the eigenvalues leads to the SRB generation.

Let us first consider the defocusing case. When $\sigma = -1$, we have $\mu|_{\gamma=0} > 0$, $\nu|_{\gamma=0} > 0$. This yields, from Eq. (8), $\chi_{AB}^{(+)} = 0$, but $\chi_{AB}^{(-)} \neq 0$ [when $(\mu - \sqrt{\nu})|_{\gamma=0} < 0$]. Only the eigenvalues χ_1, χ_2 are valid for the quasi-ABs, since χ_3, χ_4 become almost real ($\chi_{3i} \to 0$, $\chi_{4i} \to 0$), see Eqs. (9). As a result, the superposition of two quasi-ABs with eigenvalues χ_1, χ_2 can produce a vector SRB.

This should be further substantiated by considering the exact relation between the MI and the SRBs. In our previous work [28] involving 2×2 Lax matrixes, we have revealed the exact link between them. It was found that the growth rate $\mathcal{G}$ is equal to the absolute difference of group velocities of paired quasi-ABs ΔV_g. In other words, $\mathcal{G} = \gamma \Delta V_g$. However, for vector SRBs this relation is more complex. It involves specific eigenvalues of individual quasi-ABs. Namely,

$$\Delta V_g(\chi_1; \chi_2) = |V_g(\chi_1) - V_g(\chi_2)|. \quad (10)$$

By inserting (9) into (10) and omitting the higher-order terms, we have $\Delta V_g(\chi_1; \chi_2) = |(\omega/\gamma)\chi_{AB}^{(-)}|$. Comparing the expressions for $\mathcal{G}$ and ΔV_g, we have

$$\mathcal{G} = \gamma \Delta V_g(\chi_1; \chi_2). \quad (11)$$

Equation (11) describes the explicit relation between the MI and the SRBs in the defocusing case.

The main difference of vector SRBs from the SRBs of a scalar NLSE is the complex amplitude profiles in the components $\psi^{(1)}$ and $\psi^{(2)}$. These profiles differ significantly and cannot be reduced to a single function at any $\beta \neq 0$. These solutions are true vector SRBs. Only in the limit $\beta \to 0$, the two components become linearly related thus leading to the scalar SRBs. The scalar SRBs do not exist in the defocusing case as can be seen from Fig. 1(a). They can only exist in the focusing regime, as follows from the lhs panel in Fig. 1(b).

The exact SRB solutions can be constructed by performing the higher iterations of Darboux transformation. Such iteration directly leads to the nonlinear superposition of the fundamental quasi-ABs (Kth-order solutions where K is an

even number), where each breather is associated with an individual eigenvalue and free parameters $(x_{0k}, t_{0k}, \theta_k)$, $k = 1, \ldots, K$. If θ_k is fixed, the spatiotemporal distribution of such SRB strongly depends on the relative separations in both x and t, i.e., $\delta x = \{x_{01}, \ldots, x_{0K}\}$, and $\delta t = \{t_{01}, \ldots, t_{0K}\}$ [45]. They are cumbersome and will not be presented here in explicit form. Instead, we present them graphically. An alternative way to obtain them is the direct numerical simulations of Eqs. (1). By definition, the SRBs can be excited using the initial conditions in the form of periodic perturbation of the vector plane wave that is localized in x:

$$\psi^{(j)} = \psi_0^{(j)}[1 + \epsilon L_p(x/x_W) \cos(\omega x) \exp[i\phi^{(j)}]]. \quad (12)$$

The localized function L_p is either the sech-function $L_p = \text{sech}(x/x_W)$ or a Gaussian function $L_p = \exp(-x^2/x_W^2)$ with x_W being the width of the localisation. The width x_W must be comparable to that of the exact solutions, $1/(2\gamma)$. The modulation frequency ω is the same as in the exact solution while ϵ is the small amplitude ($\epsilon \ll 1$). The phases $\phi^{(j)}$ are arbitrary. We let $\phi^{(j)} = 0$. We have shown that once x_W and ω are fixed by the exact solutions, $\phi^{(j)}$ are not essential for the vector SRB excitation (see Supplemental Material [45] for more numerical simulations).

Figure 2 displays the amplitude profiles of the vector field obtained from (a) numerical simulations and (b) exact solutions for the defocusing case ($\sigma = -1$). The plane wave in (12) is unstable relative to the modulation and evolves into two dark quasi-ABs with opposite velocities. Despite using the approximate initial conditions, numerical simulations and exact solutions [$\psi^{(j)}(\chi_1; \chi_2)$] are in good agreement except for the SRB position in t. This can be seen from Fig. 2(a) as well as from the detailed comparison of the wave profiles in Fig. 2(b). Once the parameters (ω,
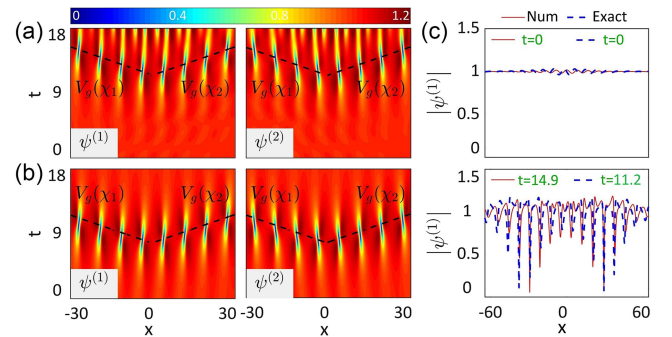

FIG. 2. Amplitude distributions of vector SRBs with $\sigma = -1$. (a) Numerical simulations started with (12), (b) Exact solution $|\psi^{(j)}(\chi_1; \chi_2)|$. Dashed lines illustrate the group velocities of individual breathers. (c) Amplitude profiles at fixed values of t in (a) and (b). Parameters are $\beta = 1$, $\gamma = 0.059$, $\omega = 0.8$, $\delta x = \{-4.8177, -2.6905\}$, $\delta t = \{0.6511, -0.0300\}$, $\theta_1 = 0$, $\theta_2 = \pi$, and $x_W = 15$, $\phi^{(j)} = 0$, $\epsilon = 0.01$.
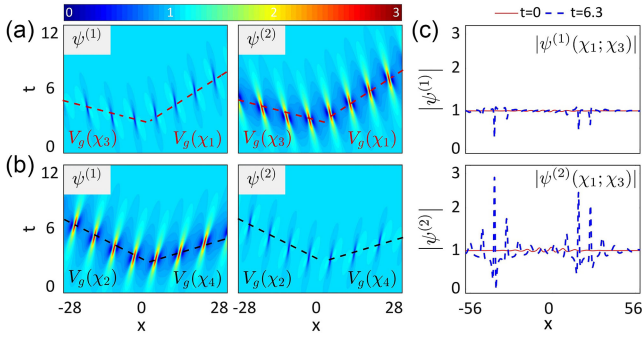
FIG. 3. Amplitude evolution of two exact solutions (a) $|\psi^{(j)}(\chi_1;\chi_3)|$ and (b) $|\psi^{(j)}(\chi_2;\chi_4)|$ of vector SRBs with $\sigma = 1$. (c) Amplitude profiles of the two field components in (a) at $t = 0$ and $t = 6.3$. Parameters are $\beta = 1$, $\gamma = 0.1$, $\omega = 0.8$, $\theta_1 = \theta_2 = 0$, $\delta x = \{-5.9118, -2.5549\}$, $\delta t = \{-1.2720, -0.7061\}$.
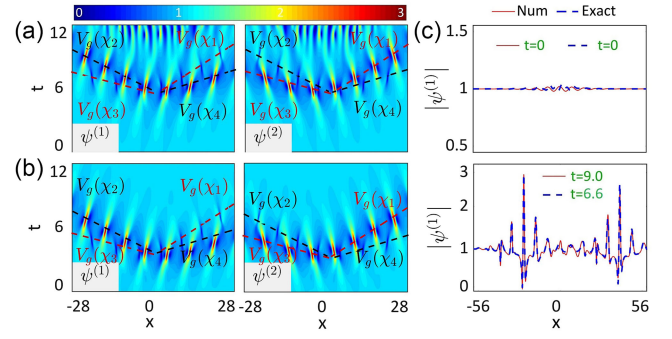

FIG. 4. Amplitude distributions of vector SRBs with $\sigma = 1$. (a) Numerical simulations started with (12). (b) Exact solution $|\psi^{(j)}(\chi_1;\chi_3;\chi_2;\chi_4)|$. (c) Amplitude profiles in (a) and (b) at $t = 0$ (upper plot) and at the points of maximal amplitudes (lower plot). Parameters are the same as in Fig. 3 but $x_W = 10$, $\phi^{(j)} = 0$, $\epsilon = 0.01$, and $\delta x_{(1,3,2,4)} = \{-5.3778, -11.5274, -8.0114, -6.3001\}$, $\delta t_{(1,3,2,4)} = \{-1.7220, 0.3178, 0.4620, -2.1747\}$.

x_W) are taken from the exact solutions, the input (12) generates the SRBs with good accuracy.

Figure 1(b) shows that the focusing regime ($\sigma = 1$) is more complicated. Here, two subcases can be distinguished: $\nu|_{\gamma=0} \geq 0$ and $\nu|_{\gamma=0} < 0$. When $\nu|_{\gamma=0} \geq 0$, only χ_1 and χ_2 are valid eigenvalues for the quasi-ABs [left panel in Fig. 1(b)]. On the contrary, when $\nu|_{\gamma=0} < 0$, all four eigenvalues (9) are valid [right panel in Fig. 1(b)]. However, not every nonlinear superposition leads to the SRB. In particular, from Eq. (9) we have

$$\Delta V_g(\chi_1;\chi_3) = \Delta V_g(\chi_2;\chi_4) = \left| \frac{\omega}{\gamma} \chi_{AB}^{(-)} \right|. \quad (13)$$

The growth rate is $\mathcal{G} = \gamma \Delta V_g(\chi_1;\chi_3) = \gamma \Delta V_g(\chi_2;\chi_4)$. Then, there are two types of SRBs sharing the same growth rate $\mathcal{G}$ for any given localized periodic modulation with the width $1/\gamma$ and the frequency ω. They correspond to the superposition of quasi-ABs either with the eigenvalues χ_1 and χ_3 or χ_2 and χ_4.

Figures 3(a) and 3(b) show the amplitude evolution of these two SRBs, $|\psi^{(j)}(\chi_1;\chi_3)|$ and $|\psi^{(j)}(\chi_2;\chi_4)|$, respectively. They demonstrate complimentary wave patterns. The SRB $|\psi^{(j)}(\chi_1;\chi_3)|$ clearly shows the two quasi-ABs with periodic dark structures in $\psi^{(1)}$ component and periodic bright structures in $\psi^{(2)}$ component. On the contrary, the SRB $|\psi^{(j)}(\chi_2;\chi_4)|$ shows periodic bright structures in $\psi^{(1)}$ component and periodic dark structures in $\psi^{(2)}$ component. The angles of propagation of individual quasi-ABs in the two superpositions correspond to their group velocities that depend on the eigenvalues. This creates an asymmetry in the SRB patterns.

More complex SRBs that involve four eigenvalues can be constructed in the focusing case. These are fourth-order solutions that are superpositions of four quasi-ABs. We denote such a solution as $\psi^{(j)}(\chi_1;\chi_3;\chi_2;\chi_4)$. The amplitudes are presented in Fig. 4(b). It can be considered as a superposition of the two types of SRBs shown in Figs. 3(a) and 3(b).

Such a solution can be also generated in numerical simulations using the same initial conditions (12) that generate lower-order SRBs. The results are shown in Fig. 4(a). The correspondence between the numerical results and exact solution requires careful adjustment of parameters. They are given in the caption to the figure. We have to mention that the excitation of such higher-order structures using the initial conditions (12) is possible only when the two lowest-order SR breathers share the same MI growth rate.

In conclusion, we presented the theory of SRBs for Manakov equations. It can be useful in practical applications and for the interpretation of experimental results. In optics, defocusing vector breathers can be observed using the platform developed in [36]. It potentially can be used to experimentally reproduce solutions from the present Letter.

[*]chongliu@nwu.edu.cn
[†]Nail.Akhmediev@anu.edu.au

[1] N. Akhmediev and A. Ankiewicz, *Solitons: Nonlinear Pulses and Beams* (Chapman and Hall, London, 1997).
[2] N. Akhmediev and A. Ankiewicz, *Dissipative Solitons, Lecture Notes in Physics* (Springer, Berlin, 2005).
[3] N. Akhmediev and A. Ankiewicz, *Dissipative Solitons: From Optics to Biology and Medicine* (Springer, Berlin, 2008).

[4] S. Flach and A. V. Gorbach, Discrete breathers—Advances in theory and applications, Phys. Rep. **467**, 1 (2008).

[5] F. Lederer, G. I. Stegeman, D. N. Christodoulides, G. Assanto, M. Segev, and Y. Silberberg, Discrete solitons in optics, Phys. Rep. **463**, 1 (2008).

[6] Y. V. Kartashov, B. A. Malomed, and L. Torner, Solitons in nonlinear lattices, Rev. Mod. Phys. **83**, 247 (2011).

[7] V. V. Konotop, J. Yang, and D. A. Zezyulin, Nonlinear waves in $\mathcal{PT}$-symmetric systems, Rev. Mod. Phys. **88**, 035002 (2016).

[8] J. M. Dudley, F. Dias, M. Erkintalo, and G. Genty, Instabilities, breathers and rogue waves in optics, Nat. Photonics **8**, 755 (2014).

[9] J. M. Dudley, G. Genty, A. Mussot, A. Chabchoub, and F. Dias, Rogue waves and analogies in optics and oceanography, Nat. Rev. Phys. **1**, 675 (2019).

[10] M. Sato, B. E. Hubbard, and A. J. Sievers, Colloquium: Nonlinear energy localization and its manipulation in micromechanical oscillator arrays, Rev. Mod. Phys. **78**, 137 (2006).

[11] H. Xiong, J. Gan, and Y. Wu, Kuznetsov-Ma soliton dynamics based on the mechanical effect of light, Phys. Rev. Lett. **119**, 153901 (2017).

[12] N. Akhmediev, A. Ankiewicz, and M. Taki, Waves that appear from nowhere and disappear without a trace, Phys. Lett. A **373**, 675 (2009).

[13] N. Akhmediev, J. Soto-Crespo, and A. Ankiewicz, Extreme waves that appear from nowhere: On the nature of rogue waves, Phys. Lett. A **373**, 2137 (2009).

[14] N. Akhmediev, J. Soto-Crespo, and A. Ankiewicz, How to excite a rogue wave, Phys. Rev. A **80**, 043818 (2009).

[15] G. Xu, A. Gelash, A. Chabchoub, V. Zakharov, and B. Kibler, Breather wave molecules, Phys. Rev. Lett. **122**, 084101 (2019).

[16] C. Liu, Z.-Y. Yang, W.-L. Yang, and N. Akhmediev, Chessboard-like spatio-temporal interference patterns and their excitation, J. Opt. Soc. Am. B **36**, 1294 (2019).

[17] J. M. Soto-Crespo, N. Devine, and N. Akhmediev, Intergrable turbulence and rogue waves: Breathers or solitons?, Phys. Rev. Lett. **116**, 103901 (2016).

[18] N. Akhmediev, V. I. Korneev, and N. V. Mitskevich, N-modulation signals in a single-mode optical waveguide under nonlinear conditions, Zh. Exp. Teor. Fiz. **94**, 159 (1988) [Sov. Phys. JETP **67**, 89 (1988)].

[19] M. Erkintalo, K. Hammani, B. Kibler, C. Finot, N. Akhmediev, J. M. Dudley, and G. Genty, Higher order modulation instability in nonlinear fiber optics, Phys. Rev. Lett. **107**, 253901 (2011).

[20] V. E. Zakharov and A. A. Gelash, Nonlinear stage of modulation instability, Phys. Rev. Lett. **111**, 054101 (2013).

[21] A. A. Gelash and V. E. Zakharov, Superregular solitonic solutions: A novel scenario for the nonlinear stage of modulation instability, Nonlinearity **27**, R1 (2014).

[22] B. Kibler, A. Chabchoub, A. Gelash, N. Akhmediev, and V. E. Zakharov, Superregular breathers in optics and hydrodynamics: Omnipresent modulation instability beyond simple periodicity, Phys. Rev. X **5**, 041026 (2015).

[23] J. H. Zhang, L. Wang, and C. Liu, Superregular breathers, characteristics of nonlinear stage of modulation instability induced by higher-order effects, Proc. R. Soc. A **473**, 20160681 (2017).

[24] C. Liu, Y. Ren, Z.-Y. Yang, and W.-L. Yang, Superregular breathers in a complex modified Korteweg–de Vries system, Chaos **27**, 083120 (2017).

[25] Y. Ren, C. Liu, Z.-Y. Yang, and W.-L. Yang, Polariton superregular breathers in a resonant erbium-doped fiber, Phys. Rev. E **98**, 062223 (2018).

[26] Y. Ren, X. Wang, C. Liu, Z.-Y. Yang, and W.-L. Yang, Characteristics of fundamental and superregular modes in a multiple self-induced transparency system, Commun. Nonlinear Sci. Numer. Simul. **63**, 161 (2018).

[27] C. Liu and N. Akhmediev, Super-regular breathers in nonlinear systems with self-steepening effect, Phys. Rev. E **100**, 062201 (2019).

[28] C. Liu, Z.-Y. Yang, and W.-L. Yang, Growth rate of modulation instability driven by superregular breathers, Chaos **28**, 083110 (2018).

[29] A. A. Gelash, Formation of rogue waves from the locally perturbed condensate, Phys. Rev. E **97**, 022208 (2018).

[30] M. Conforti, S. Li, G. Biondini, and S. Trillo, Automodulation versus breathers in the nonlinear stage of modulational instability, Opt. Lett. **43**, 5291 (2018).

[31] S. Trillo and M. Conforti, Quantitative approach to breather pair appearance in nonlinear modulational instability, Opt. Lett. **44**, 4275 (2019).

[32] S. V. Manakov, On the theory of two-dimensional stationary self-focusing of electromagnetic waves, Sov. Phys. JETP **38**, 248 (1974).

[33] P. G. Kevrekidis, D. Frantzeskakis, and R. Carretero-Gonzalez, *Emergent Nonlinear Phenomena in Bose-Einstein Condensates: Theory and Experiment* (Springer, Berlin Heidelberg, 2009).

[34] G. Agrawal, *Nonlinear Fiber Optics*, 5th ed. (Academic Press, San Diego, 2012).

[35] J. U. Kang, G. I. Stegeman, J. S. Aitchison, and N. Akhmediev, Observation of Manakov spatial solitons in AlGaAs planar waveguides, Phys. Rev. Lett. **76**, 3699 (1996).

[36] B. Frisquet, B. Kibler, P. Morin, F. Baronio, M. Conforti, G. Millot, and S. Wabnitz, Optical dark rogue waves, Sci. Rep. **6**, 20785 (2016).

[37] M. Onorato, A. R. Osborne, and M. Serio, Modulational instability in crossing sea states: A possible mechanism for the formation of freak waves, Phys. Rev. Lett. **96**, 014503 (2006).

[38] Z. Yan, Vector financial rogue waves, Phys. Lett. A **375**, 4274 (2011).

[39] A. Degasperis and S. Lombardo, Integrability in action: Solitons, instability and rogue waves, in *Rogue and Shock Waves in Nonlinear Dispersive Media*, edited by M. Onorato, S. Residori, and F. Baronio (Springer, New York, 2016).

[40] F. Baronio, M. Conforti, A. Degasperis, S. Lombardo, M. Onorato, and S. Wabnitz, Vector rogue waves and baseband modulation instability in the defocusing regime, Phys. Rev. Lett. **113**, 034101 (2014).

[41] H.-Y. Tian, B. Tian, Y.-Q. Yuan, and C.-R. Zhang, Super-regular solutions for a coupled nonlinear Schrödinger system in a two-mode nonlinear fiber, Phys. Scr. **96**, 045213 (2021).

[42] A. Gelash and A. Raskovalov, Vector breathers in the Manakov system, Stud. Appl. Math. **150**, 841 (2023).

[43] D. Kraus, G. Biondini, and G. Kovačič, The focusing Manakov system with nonzero boundary conditions, Nonlinearity **28**, 3101 (2015).

[44] V. B. Matveev and M. A. Salle, *Darboux Transformations and Solitons*, Series in Nonlinear Dynamics (Springer Verlag, Berlin, 1991).

[45] See Supplemental Material at http://link.aps.org/supplemental/10.1103/PhysRevLett.132.027201 for details.

[46] S.-C. Chen, C. Liu, X. Yao, L.-C. Zhao, and N. Akhmediev, Extreme spectral asymmetry of Akhmediev breathers and Fermi-Pasta-Ulam recurrence in a Manakov system, Phys. Rev. E **104**, 024215 (2021).

[47] C. Liu, S.-C. Chen, X. Yao, and N. Akhmediev, Modulation instability and non-degenerate Akhmediev breathers of Manakov equations, Chin. Phys. Lett. **39**, 094201 (2022).

[48] S.-C. Chen and C. Liu, Hidden Akhmediev breathers and vector modulation instability in the defocusing regime, Physica (Amsterdam) **438D**, 133364 (2022).

[49] C. Liu, S.-C. Chen, X. Yao, and N. Akhmediev, Non-degenerate multi-rogue waves and easy ways of their excitation, Physica (Amsterdam) **433D**, 133192 (2022).

[50] W.-J. Che, S.-C. Chen, C. Liu, L.-C. Zhao, and N. Akhmediev, Nondegenerate Kuznetsov-Ma solitons of Manakov equations and their physical spectra, Phys. Rev. A **105**, 043526 (2022).

[51] S.-C. Chen, C. Liu, and N. Akhmediev, Higher-order modulation instability and multi-Akhmediev breathers of Manakov equations: Frequency jumps over the stable gaps between the instability bands, Phys. Rev. A **107**, 063507 (2023).

[52] W.-J. Che, C. Liu, and N. Akhmediev, Fundamental and second-order dark soliton 2 solutions of 2- and 3-component Manakov equations in the defocusing regime, Phys. Rev. E **107**, 054206 (2023).

[53] E. A. Kuznetsov, Solitons in a parametrically unstable plasma, Sov. Phys. Dokl. **22**, 575 (1977); Y. C. Ma, The Perturbed plane wave solutions of the cubic nonlinear Schrödinger equation, Stud. Appl. Math. **60**, 43 (1979).

[54] N. Akhmediev and V. I. Korneev, Modulation instability and periodic solutions of the nonlinear Schrödinger equation, Theor. Math. Phys. **69**, 1089 (1986).

[55] D. H. Peregrine, Water waves, nonlinear Schrödinger equations and their solutions, J. Aust. Math. Soc. Series B, Appl. Math. **25**, 16 (1983).

[56] L. Ling and L.-C. Zhao, Modulational instability and homoclinic orbit solutions in vector nonlinear Schrödinger equation, Commun. Nonlinear Sci. Numer. Simul. **63**, 161 (2018).